Optical Far-IR wave Generation - An ESA review study

B. Leone [1], V. Krozer [2], M. Feiginov [3], H. Roskos [4], H. Quast [4], T. Löffler [4], G. Loata [4], G. Döhler [5], P. Kiesel [5], M. Eckardt [5], A, Schwanhäußer [5], T. O. Klaassen [6], P. Lugli [7]

[1] ESA Directorate of Technical and Operational Support, ESTEC, Noordwijk, The Netherlands
[2] Denmark Technical University, Lyngby, Denmark
[3] Technical University of Darmstadt, Darmstadt, Germany
[4] University of Frankfurt, Frankfurt, Germany
[5] University of Erlangen, Erlangen, Germany
[6] Delft University of Technology, Delft, The Netherlands
[7] University of Rome "Tor Vergata", Rome, Italy

Abstract

A study initiated by the European Space Agency was recently concluded, which aimed at identifying the most promising technologies to significantly improve on the generation of coherent electromagnetic radiation in the THz regime for space applications. The desired improvements include, amongst others, higher output powers and efficiencies at increasingly higher frequencies, wider tunability and, possibly, miniaturization.

As the title of the paper suggests, the baseline technologies considered from the start in this study revolved around optical schemes, such as photomixing, compared to all electronic techniques. However, emphasis was put on conducting a perusal of any scheme found in the literature and performing an overall comparison with a fixed set of criteria. To this end, a number of universities and research institutes were involved to allow for a sufficient coverage of all relevant technical and research areas and, thus, ensure a review of both current and emerging technologies in this field that would be as thorough and complete as possible.

The review study combined published results and mathematical modelling in order to determine the theoretical performance limitations of a given technology and/or scheme. The basic requirements to help crystallize selection criteria were, broadly speaking: power performance, linewidth, tunability and space worthiness in the frequency range ~1 to 3 THz.

Some of the most significant findings will be presented together with the two technologies selected for medium to short term development. These are a scheme using advanced p-i-n photomixer superlattice structures and, reflecting recent results, THz Quantum Cascade Laser technology.

Introduction

Several Terahertz heterodyne technology development activities have been initiated and funded in the past years by the European Space Agency (ESA) mainly in response to the technological needs of the Herschel Observatory mission. Several of these activities are still ongoing and were well represented at this conference [1–8].
These include:

- Superconducting mixer development [1–4]
- Multipixel heterodyne HEB receiver [6]
- Far-IR optics design and verification tools [5]
- Optical Far-IR wave generation

This paper deals with the last activity, which is complementary to the mixer development activities. In particular, any multipixel heterodyne receiver requires considerable LO power if the same source is used for several pixels. Presently, there exists no compact THz source to do this. Therefore, the development of compact, Spaceworthy, high power sources is considered by ESA as an enabling technology for instruments incorporating THz mixer arrays. The title of the development activity pointed from the outset that this should be achieved by optical means. Indeed, this was also a conclusion of the study.

Study Rationale

The optical Far-IR wave generation activity was split into two phases. In the first phsse, current technologies were reviewed from available scientific literature and their potential analysed in turn using modelling and first principle calculations. In the second phase the most promising technologies will be developed.
The first phase was articulated according to a set of tasks summarized as follows:

- Establish the theoretical limit for the maximum output power from multipliers at the frequencies under consideration,
- Survey and assess the various novel techniques for the generation of THz power,
- Demonstrate the experimentally achievable capabilities of photo-mixer devices based on LT GaAs, p-i-n diodes, and of lasers for THz power generation,
- Survey and assess the measurement, characterisation and system techniques and requirements for optical far-infrared power generation, and
- Outline the technological development plan and a detailed technological roadmap for the most promising technology.

In this phase two competing research consortia were contracted to perform the review in parallel. One consortium is represented by the co-authors of this paper; the Rutherford Appleton Laboratory led the other consortium. At the end of this first phase, only one of the two consortia would be selected to continue the actual technology development on grounds of the novelty of the selected optical THz technology or scheme. This way, the quality of the review was ensured through competitiveness.

Here, only the results of the winning consortium will be presented. This will not affect the completeness of the results since most conclusions regarding existing technologies were similar for both consortia and only the conclusions on the implementation of the technology roadmap differ.
The second phase is currently ongoing and focuses on development of the most promising technologies selected in the first phase according to a development roadmap.

Summary of Results

The selection criteria used in the review reflected both the desired characteristics of an ideal THz source for space applications as well as the actual technologies considered in the study. Without loss of generality, however, one can summarize the following list of criteria:

- Maximum output power
- Conversion (optical) efficiency
- Electrical efficiency
- Maximum output frequency
- Frequency stability
- Linewidth
- Spectral purity
- Tunability
- Operating conditions (temperature, current, voltage, magnetic field, vacuum, etc…)
- Coupling issues
- Miniaturization
- Space qualifiability

The current state-of-the-art THz source technology for space is represented by solid-state frequency multiplication. Therefore, the theoretical limit of multiplier circuits with Schottky varactor diodes were established in this study by simulation and the simulated results were subsequently used for comparison with experimental results from photomixing and laser experiments. Although impressive results have been demonstrated up to almost 2 THz [9–10], the resulting efficiencies and output powers are really only sufficient to drive single pixel mixers rather than mixer arrays. Furthermore, efficiency plummets at higher frequencies such that is believed to be difficult to push these results above 2.5 THz. This is due to the fact that the doping concentrations for the Schottky varactor devices employed in these multipliers ought to be well above $1 .10^{17} /cm^3$. At these doping levels the contribution of the parasitic tunneling current becomes large and the C_{max}/C_{min} ratio is lowered. Consequently, the efficiency rapidly deteriorates.

Furthermore, a large number of other known and published techniques for the generation of THz power, with special emphasis on their CW THz power capabilities have also been considered in the study but have been rejected from the technology development roadmap, at least for the time being, on the basis of their shortcomings with respect to selec-

tion criteria listed above. In the following sections these results will not be presented for brevity's sake.

In summary, the technologies selected for the development roadmap are optical photomixing and direct THz laser generation. The state-of-the-art in the area of photomixing is currently set by two device concepts, namely the LTGaAs MSM structures and the p-i-n diode structures. Both device concepts have already demonstrated the working principle but are still far from the requirements in output power for receiver applications at THz frequencies. These techniques and the other published in the literature will be considered in this study report.
Direct generation of THz power with either Quantum Cascade Laser structures or p-Ge lasers was also thought to be very promising. In particular THz QCLs have been introduced only recently and their potential in performance, especially for operation in the higher end of the THz frequency range, is of great interest in the preparation of new applications.

Introduction to Photomixers

The generation of high frequency radiation by photomixing is based on generating periodically charge carriers in a semiconductor by two lasers emitting at nearly the same photon frequencies ν_0, detuned by the beat frequency ν_{THz}. If these photo-generated carriers are subjected to a DC electric field F_0 applied between two contacts connected to an antenna, a THz current $I_{THz}(t)$ is induced by the photo-generated carriers, which, depending on the load represented by the antenna, leads also to an AC voltage $U_{THz}(t)$ at the contacts. If the beat frequency is low compared to the inverse carrier transport time $1/\tau$, the AC current and voltage will follow the carrier generation fully in phase with the beat frequency and with an amplitude,

$$I^0 = e\,(dN/dt) = e\,\eta_{ph}\,(P_L/h\nu_0) \qquad (1)$$

Here, e stands for the elementary charge, dN/dt is the electron-hole pair generation rate, which is equal to the average photon absorption rate $\eta_{ph}\,P_L/h\nu_0$; P_L is the laser power, $h\nu_0$ the lasers photon energy and η_{ph} the fraction of incident photons absorbed in the active part of the mixer. The "carrier transport time" can be either the transit time between the contacts or the recombination lifetime. Assuming reasonable values for the high-field drift velocities v_{dr} of electrons and holes of the order of 10^7 cm/s and contact separations L of the order of a μm, we expect transit times $\tau_{tr} = L/v_{dr}$ of the order of 10 ps, i.e. the condition for maximum AC photocurrent is fulfilled only if the beat frequency is << 1/10ps = 100 GHz. In general, when this condition is not fulfilled it can be shown that the following relation relates the AC current to the average current:

$$I_{THz}(t) = I^0\,(1+2\pi i\nu_{THz}\tau_{tr})^{-1}\cos(2\pi\nu_{THz}t) = e\,\eta_{ph}\,(P_L/h\nu_0)\,(1+2\pi i\nu_{THz}\tau_{tr})^{-1}\cos(2\pi\nu_{THz}t) \qquad (2)$$

Thus, at THz-frequencies the amplitude of the THz-current I_{THz}^{0} is much smaller than I^0. At first glance, the situation would *seem* to improve drastically, if the carrier transport time were to become much smaller than the transit time. This happens if transit times are limited due to the recombination lifetime $\tau_{rec} << \tau_{tr}$, so that τ_{rec} replaces τ_{tr} in Equ. (2). However, in this case each photo-generated carrier no longer contributes the same amount to I^0, as its drift length $l_{dr} = v_{dr}\tau_{rec}$ is now only the fraction l_{dr} /L, i.e., the photo-conductive "gain" $g = l_{dr}/L = (\tau_{rec}/\tau_{tr})$ becomes << 1.
Now, by replacing the expression for I^0 given in Equ. (1) by the following,

$$I^0 = e\,(dN/dt)\,(v\tau/L) = e\,\eta_{ph}\,(P_L/h\nu_0)\,(\tau_{rec}/\tau_{tr}) \tag{3}$$

into Equ. (2), one finds that

$$I_{THz}(t) = I^0\,(1+2\pi i\nu_{THz}\tau_{rec})^{-1}\cos(2\pi\nu_{THz}t) = e\,\eta_{ph}\,(P_L/h\nu_0)\,(\tau_{rec}/\tau_{tr})\,(1+2\pi i\nu_{THz}\tau_{rec})^{-1}\cos(2\pi\nu_{THz}t) \tag{4}$$

We see that for $\tau_{rec} << \tau_{tr}$: (i) the 3dB-frequency becomes much larger, i.e. $\nu_{3dB} = 1/2\pi\tau_{rec}$, instead of $\nu_{3dB} = 1/2\pi\tau_{tr}$, (ii) the amplitude of the AC current for $\nu_{THz} >> \nu_{3dB}$ given by $I_{THz}^{0} = e\,\eta_{ph}\,(P_L/h\nu_0)\,(2\pi\nu_{THz}\tau_{tr})^{-1}$ is unchanged, whereas (iii) the DC current I^0 is strongly reduced by $g = l_{dr}/L = (\tau_{rec}/\tau_{tr})$.

For arbitrary ν_{THz} the emitted THz power can be estimated by,

$$P_{THz} = \tfrac{1}{2}\,(I_{THz}^{0})^2\,R_a = \tfrac{1}{2}\,\{e\,\eta_{ph}\,(P_L/h\nu_0)\}^2\,(\tau_{rec}/\tau_{tr})^2\,[1+(2\pi\nu_{THz}\tau_{rec})^2]^{-1}\,R_a = P_{THz}^{id}\,(\tau_{rec}/\tau_{tr})^2/[1+(2\pi\nu_{THz}\tau_{rec})^2] \tag{5}$$

where,

$$P_{THz}^{id} = \tfrac{1}{2}\,\{e\,\eta_{ph}\,(P_L/h\nu_0)\}^2\,R_a \tag{6}$$

corresponds to the THz-power emitted by an ideal photomixer, assuming $\eta_{ph} = 1$. R_a is the radiative resistance of the antenna, which is typically in the order of 50 to 100 Ω. For an ideal GaAs photomixer (with $h\nu_0 = 1.43$ eV $\approx E_g$) the following values are expected: $R_a = 70\ \Omega$ and $P_L = 10$ mW value of $P_{THz}^{id} = 1.7$ mW, corresponding to a conversion efficiency $\eta_{THz} = P_{THz}/P_L = 17$ %.

Assessment of Photoconductors

LT-GaAs is used in *photoconductive* photomixers because of the short electron and hole capturing and recombination lifetime. Minimum values of $\tau_{rec} = 130$ fs have been reported, corresponding to a 3dB frequency of 1.2 THz. In optimized LT-GaAs-photomixers the photoconductive area consists of an LT-GaAs-layer with a thickness of the order of 1 μm and an interdigitated contact structure with contact separations of L =

1.8 μm, covering a quadratic area of 8 x 8 μm^2. Using again $v_{dr} = 10^7$ cm/s we obtain τ_{tr} = 18 ps. The maximum laser power is typically about P_L = 100 mW. With these values Equ. (5) yields, at 1 THz, a value of P_{THz}^{th} = 170mW $(0.130ps/18ps)^2/(1+0.67)$ = 5 μW, or an optical conversion efficiency of $\eta_{THz}^{th} = 5 \times 10^{-5}$. These values are rather close to the best-reported experimental values of P_{THz}^{exp} = 2 μW and $\eta_{THz}^{exp} = 2 \times 10^{-5}$, respectively [11]. It should be noted that, although in this case ν_{THz} is slightly smaller than ν_{3dB}, the low efficiency at this frequency does not result primarily from the short recombination lifetime, but rather from the long transit time. For $\tau_{rec} >> 130$ fs, Equ. (5) yields only a slightly higher value of $P_{THz} = P_{THz}^{id} (1/2\pi\nu_{THz}\tau_{tr})^2$ = 13 μW.

In fact, the real advantage of the short recombination lifetime is the reduction of the steady-state carrier density at such high laser power. A simple estimate yields an average photo-induced carrier density in the LT-GaAs layer of about $10^{15} cm^{-3}$ for the present example. Although seemingly small this carrier density tends to screen the electric fields between the contacts, thus lowering the photocurrent, provided that the drift velocities of electrons and holes are not equal. Even if the steady state carrier density were determined by an ideal carrier transit time of about 20 ps, the photo-induced carrier density would be larger than $10^{17} cm^{-3}$. In this case, even extremely high external voltages would be nearly completely screened by space charge building up near the contacts.

Inspection of Equ. (5) suggests that the most promising approach for improving on the performance of photomixers might be a reduction of the transit time by reducing the contact separation L. Unfortunately, a reduction of L, while keeping the active area constant, results in an increase of the capacitance approximately proportional to L^{-2}. Taking into account that the present example represents already the design where the RC-3dB frequency $\nu_{RC} = 1/2\pi R_a C_{LT} \approx 1$THz ($C_{LT}$ is the capacitance of the LT-GaAs layer with the interdigitated contacts) this implies a superlinear roll-off of the AC current I_{THz} with decreasing L which overcompensates the expected linear increase.

These simple theoretical design considerations are supported by the empirical observation that in spite of significant efforts no fundamental improvement of performance has been achieved in the field of LT-GaAs photomixers during the past years. In principle, the RC-roll-off problem can be overcome by taking advantage of the traveling wave concept. At suitably chosen angle of incidence of the photomixing lasers the interference pattern and, thus, the phase of maximum photocurrent generation can propagate with the same speed as the THz mixing signal in an active transmission line with LT-GaAs in between [12–15].

Assessment of Photodiodes

Similar considerations as outlined above can be applied also to p-i-n photomixers. One obtains the ideal value for the emitted THz power, according to Equ. (6) if the amplitude of the AC current, I_{THz}^0, is affected neither by the RC nor by the transit time roll-off, pro-

vided that $\eta_{ph}=1$. In the general case the product of the corresponding roll-off factors reduces the emitted power:

$$P_{THz} = \tfrac{1}{2} (I_{THz}^{0})^2 R_a [1+(\nu_{THz}/\nu_{RC})^2]^{-1} = P_{THz}^{id} [1+(\nu_{THz}/\nu_{RC})^2]^{-1} [1+(\nu_{THz}/\nu_{tr})^2]^{-1} \quad (7)$$

The RC-3dB frequency $\nu_{RC} = 1/(2\pi\tau_{RC}) = 1/(2\pi R_a C_{pin})$ (with $C_{pin} = \varepsilon L_x L_y/4\pi L_z$ and ε = dielectric constant) scales linearly with the i-layer thickness L_z and inversely with the sample cross section. Thus *large* L_z and small cross section appear attractive. On the other hand, the transit time 3dB-frequency $\nu_{tr} \approx 1/2\tau_{tr}$ increases with the transit times becoming short. Thus, *small* values of L_z appear attractive. An optimum value of L_z for a pin photomixer can be determined from the condition $\nu_{RC} = \nu_{tr}$. The transit time is (conventionally) determined by $\tau_{tr} = L_z/v_{dr}$, where for typical fields $v_{dr} = v_{sat} = 10^7$cm/s is taken for electrons in GaAs, as the electrons are traveling at the (nearly field independent) saturation velocity v_{sat}, whereas $v_{dr} = \mu_h F$ is taken for the holes. Taking $v_{dr} = 10^7$cm/s for electrons and holes and assuming a reasonable minimum value of the cross section ($L_x = L_y = 5$ µm) we obtain $L_z^{opt} = 0.33$ µm and $\nu^{opt} = 150$ GHz. According to Equ. (7) the emitted THz power is then expected to be a factor of 4 less than P_{THz}^{id}. At 1 THz the emitted THz power should be still about 0.05 % of the ideal value. A major limitation of pin-photomixers is due to field screening effects. As the photo-generated electrons and holes drift towards the n- and the p-layers, respectively, with transit times in the ps range, a stationary space charge distribution – changing from positive sign near the p-layer to negative sign towards the n-layer – builds up in the i-layer. In order to maintain a sufficiently high field for the fast transport throughout the whole i-layer an increasingly large reverse bias is required if the laser power increases. In our case about 10 V reverse bias are necessary for $P_L = 100$ mW. With a photocurrent of 70 mA a dissipated electrical power of 700 mW (!) would result. With $R_a = 70\ \Omega$, e.g., a value of $P_{THz} = 75$ µW, would be obtained, which would represent a drastic improvement by 1 to 1 ½ orders of magnitude compared to the theoretical or the best experimental LT-photomixer results, respectively.

There are only a few reports on pin photomixers found in the literature. The best results reported are 2mW @ 100 GHz and 100 nW @ 0.625 THz achieved with 100 mW laser power [16–17]. More recently, 17 mW @ 120GHz was obtained [18].

Novel n-i-pn-i-p Superlattice Photodiode Concept

As the current in photomixers is uni-directional, the transport time ideally should be less

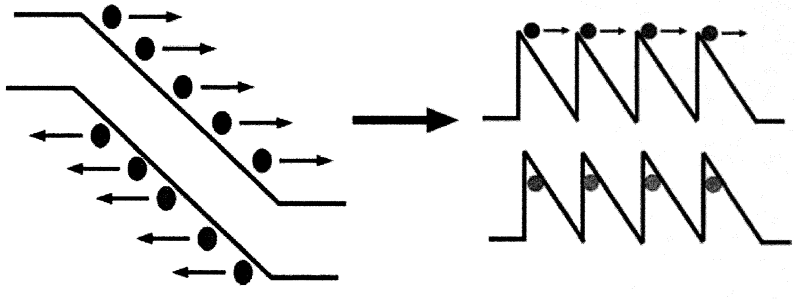

Figure 1: In order to reduce the drift length but keeping the capacitance of the whole structure constant, the pin-diode is subdivided into N nano - pin-diodes.

than about one half of the THz period, i.e. $\tau_{tr} < T_{THz}/2$. As these times are in the fs range, this implies that for the time of interest the transport can be ballistic. During this time electrons acquire a velocity strongly exceeding the high-field drift velocity and, consequently, contribute a much larger amount to the current and propagate over a longer distance. As transport for times > $T_{THz}/2$ is counterproductive it is advantageous if the electrons are stopped after a time of about $T_{THz}/2$. As (ballistic) holes are much slower, it is desirable that transport is mainly carried by the electrons. To a good approximation ballistic electron transport in the uniform electric field of a pin diode can be described by a velocity linearly increasing in time until the minimum energy for scattering into higher side valleys, $\Delta E_{\Gamma L} \approx 250$ meV in the case of GaAs, is reached. The average velocity is $v_{bal} = v_{max}/2 = 5 \times 10^7$cm/s with v_{max} determined from $m_c v_{max}^2/2 = \Delta E_{\Gamma L}$ (where m_c stands for the effective conduction electron mass in the Γ-valley). As v_{bal} is by a factor of 5 higher as v_{sat}, for a given flight time of $T_{THz}/2$ the electrons travel over correspondingly larger distances $l_z = v_{bal} T_{THz}/2 = v_{bal}/(2\nu_{THz})$. For $\nu_{THz} = 1$ THz, e.g., we obtain $l_z = 250$ nm. In order to avoid that the capacitance becomes too high and, hence, the RC–3dB frequency too low, we keep L_z sufficiently large to assure that $\nu_{3dBt} \geq \nu_{THz}$ by subdividing L_z into a superlattice consisting of N nano – p-i-n diodes of length l_z, i.e. $L_z = N\, l_z$, as shown schematically in Fig. 1. As the photo-generated carriers are now distributed over N superlattice periods the AC current amplitude I_{THz}^0 is reduced by a factor of N. Hence,

$$P_{THz} = P_{THz}^{id} N^{-2} [1+(\nu_{THz}/\nu_{RC})^2]^{-1} [1+(\nu_{THz}/\nu_{tr})^2]^{-1}. \quad (8)$$

For a given THz-frequency, ν_{THz}, the optimized number of superlattice periods, N^{opt}, is obtained from the conditions $\nu_{RC} = \nu_{THz}$ and $\nu_{tr} = \nu_{THz}$. For a superlattice of N periods ν_{RC} is given by $\nu_{3dB} = 1/(2\pi R_a C_{tot})$ with

$$C_{tot} = \varepsilon L_x L_y/(4\pi N l_z) = \nu_{THz} \varepsilon L_x L_y/(2\pi N v_{bal}), \quad (9)$$

which yields, together with $\nu_{tr} = 1/2\tau_{tr} = v_{bal}/2l_z$

$$N^{opt} = (\nu_{THz})^2 R_a \varepsilon L_x L_y / v_{bal} \quad (10)$$

and

$$P_{THz}^{opt} = \tfrac{1}{2} (e\, \eta_{ph}\, P_L/h\nu_0)^2\, R_a / (2N^{opt})^{-2} = \tfrac{1}{2} (e\, \eta_{ph}\, P_L/h\nu_0)^2\, v_{bal}^2/[4R_a (\nu_{THz}^2 \varepsilon L_x L_y)^2] \quad (11)$$

Equ. (11) suggests that the THz power increases quadratically with the laser power and decreases with the 4-th power of the THz frequency and quadratically with the cross section of the mixer. For sufficiently high values of ν_{THz} the emitted THz power is, in fact, limited only by the maximum laser power, which can be dissipated by the mixer and the minimum device dimensions L_x and L_y that can be achieved. In the range of 1 THz, however, the minimum cross section at a given laser power is limited by the maximum tolerable field changes in the i-layer, where the ballistic transport takes place. This field change is proportional to the laser power and inversely proportional to the THz fre-

quency, the number of periods and the capacitance. Using Equ.s (9) and (10) for C_{tot} and N^{opt} we see that ultimately the field changes are proportional to $P_L(L_xL_y)^{-2}\nu_{THz}^{-4}$.
For our estimates we take P_L=100 mW (as typically used in the LT-GaAs photomixing experiments; the n-i-pn-i-p photomixer can most probably tolerate even higher power, as no external voltage is to be applied to these devices, in contrast to the LT-GaAs photomixers, where the high voltage at the Schottky contacts is the origin of thermal failure near P_L exceeding 100 mW). At ν_{THz} = 1 THz one finds l_z^{opt} = 250 nm. The condition that periodic field changes should be less than ± 25 % yields $L_x = L_y$ = 9 μm and N^{opt} = 10. According to Equ. (11) one finds P_{THz} = 425 μW. For ν_{THz} = 3 THz one finds l_z = 93 nm. At this frequency the periodic field changes turn out to be far below the critical values, even if the dimensions are reduced to $L_x = L_y$ = 5 μm (the smallest values which can be achieved "easily"). In this case one finds N^{opt} = 28 and P_{THz} = 54 μW.

For the realization of the concept one has to bear in mind:

1) The transport should predominantly be carried by the (light, and therefore fast) electrons

2) The potential drop between the starting and arrival point of the electrons should be of the order of the energy difference $\Delta_{\Gamma L}$ between Γ- and L-valley (in case of GaAs).

3) Although after arrival the velocity of the carriers is zero the electrons at the minimum of the conduction band have to recombine fast enough with the holes at the valence band maximum in the neighboring n-i-p-diode (See Fig.1) in order to avoid too much carrier accumulation.

4) Although we discuss here only the example of GaAs-based photomixers other compound semiconductors (like InGaAs) have even more favorable properties regarding v_{bal} and the critical energies for scattering into side valleys $\Delta_{\Gamma L}$ or $\Delta_{\Gamma X}$.

In Fig. 2 one period of the proposed "n-i-pn-i-p superlattice" structure, designed to meet these requirements is shown. The individual "n-i-p-electron – transport diodes" which are designed to have the optimum length l_e for the ballistic electron transport and a short

transport length l_h for the holes for the chosen THz-frequency are connected to each

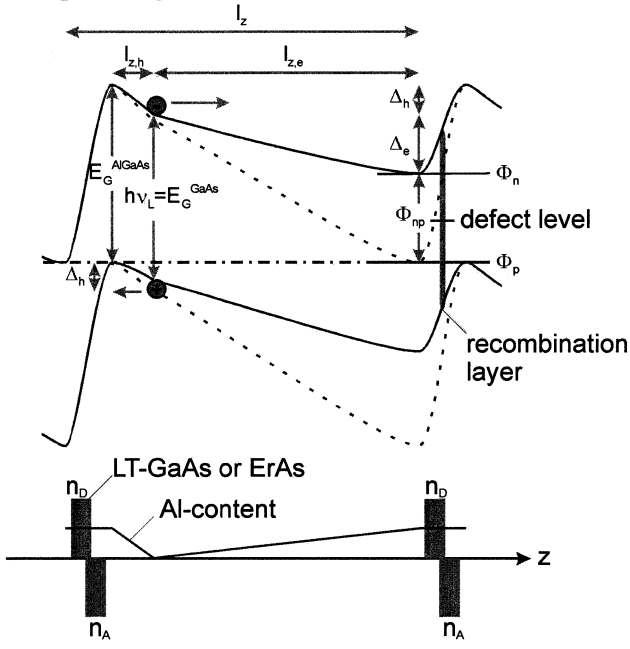

Figure 2: Band diagram, Al-content and doping profile of one period of the n-i-pn-i-p-superlattice

other by "recombination pn-junctions". These junctions are highly doped and contain a thin electron-hole recombination layer composed of either LT-GaAs or ErAs [19] and will be discussed in more detail below. The Al-content is asymmetrically graded in the i-layers (see Fig.2). Because of the varying band gap in the i-layer the electron generation takes mainly place near the point of minimum band gap as indicated in Fig.2, if the laser photon energy is suitably chosen. In Fig. 2 the band diagrams are shown for both the ground state and the excited state at illumination with high excitation energy. The ground state (dotted lines) is characterized by a common Fermi level in the n- and the p-layers. The sheet electron and hole density in the ground state is $n_0^{(2)}$ and $p_0^{(2)}$, respectively. As the photo-generated electrons and holes do not recombine instantaneously an additional sheet electron and hole density $\Delta n^{(2)} = \Delta p^{(2)}$ builds up under illumination. This space charge partially screens the built-in potential. This results in a splitting of the quasi-Fermi levels for the electrons in the n-layers and the holes in the p-layers $\phi_{np} = \phi_n - \phi_p$ (full lines in Fig. 2). Under photomixing conditions the average photocurrent generated per period of the n-i-pn-i-p superlattice, I^0/N, is flowing through the recombination diode as a (nearly constant) recombination current. The value of ϕ_{np} und thus also the potential drop within the "n-i-p electron – transport diodes" and the "np recombination diodes" corresponds to eU_{np} , where U_{np} stands for the forward bias at which just this current I^0/N is flowing in the "pn recombination diode". Under ideal operation conditions

the average value of $\phi_{np} = eU_{np}$ should be somewhat larger than $Eg - \Delta_{\Gamma L}$ and the amplitude of the (THz)-periodic variation of ϕ_{np} should be significantly smaller than ϕ_{np}, as discussed in the paragraph following Equ. (11).

Simple estimates show that depending on the laser power and the number of periods the current density in our devices will be in the order of j_{av} =1 to 100 kA/cm^2 because of the small cross sectional area L_xL_y, required according to Equ.s (9) to (11). As these values are required for a photo-induced Fermi level splitting of $\phi_{np} = eU_{np} \approx 1$ eV these values turn out to be by many orders of magnitude larger than in standard pn-junctions. Therefore, special "pn recombination diodes" have to be used, as shown in Fig. 2. In Fig. 3 the measured current density vs voltage curves for strongly doped p-n diodes with a 1.2 monolayer thick ErAs recombination layer at the interface and $n_D = 5 * 10^{18}$ cm^{-3} and $n_A = 2 * 10^{19}$ cm^{-3} are compared with reference diodes with the same doping densities, but without ErAs recombination layer. We see, that using this trick, the required high current densities are, in fact, accessible at the required excitation level.

In order to support our simple estimates from Section 4 we show in Fig. 4 the results of Monte Carlo calculations for the transient high-field transport in bulk material. From this figure it can be seen, that our estimates regarding the average ballistic velocity v_{bal}, the transport time and distance, τ_{tr} and l_z, respectively are quite realistic. In particular, we see that the position of the electrons after a given time of flight does not depend too critically on the actual field.

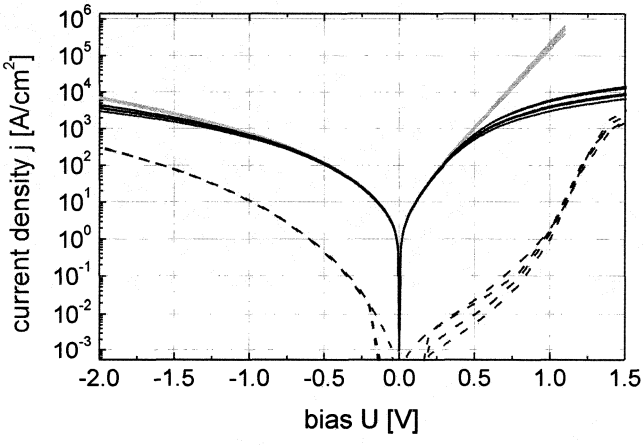

Figure 3. current density vs. voltage curves of highly doped pn-junctions without (dashed) and with ErAs recombination layer. Recombination diode (with ErAs-layer): black lines = measured, grey lines = corrected for contact layer series resistance; reference diode (without ErAs-layer): dashed line.

The distance reached after 0.5 ps, e.g., is nearly the same, if the field changes between 10 and 20 kV/cm. Recent fs- studies of the transient transport in similar nanostructures have quantitatively confirmed our Monte Carlo simulations [20–21].

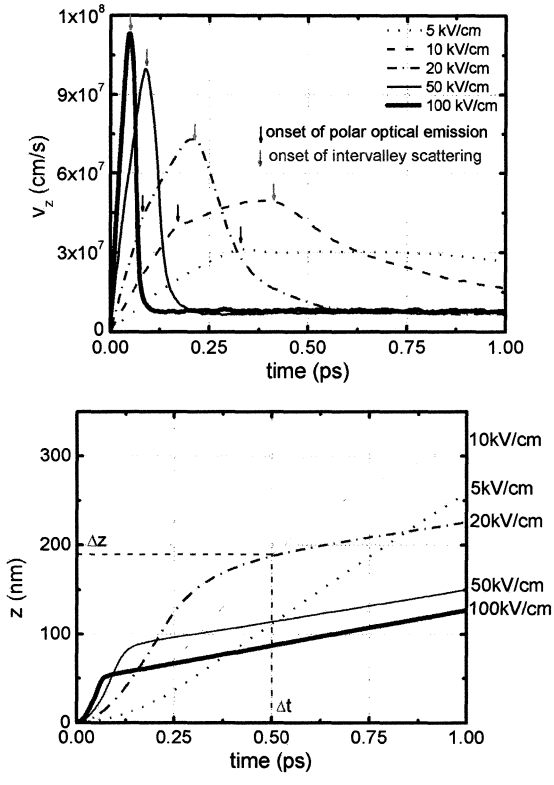

Figure 4: Monte Carlo results velocity and position vs time.

We conclude that the main drawbacks of conventional LT-GaAs based photomixers as THz-sources result from the low photoconductive gain. Our approach based on ballistic transport in a n-i-pn-i-p superlattice, in contrast, yields optimized THz-currents and THz-voltages. Impedance matching to the antenna can be achieved by suitable choice of the number of periods N of the superlattice. Moreover, this approach overcomes the usual problem of the frequency limitation due to the carrier lifetime in LT-GaAs. Therefore, particularly interesting results are expected at frequencies up to about 3 THz.

Quantum Cascade Lasers

Quantum cascade lasers are unipolar lasers that exploit the radiative transitions between two subbands of a multi quantum well system [22] or two minibands of a superlattice [23]. The basic cell is composed of an injector and an active region. The injector, usually doped, provides electrons to the upper level of the active region. Under sufficiently high electric fields, a population inversion builds up between such upper level and the lower one, which in turn depletes itself via non-radiative transitions with the level(s) of the ac-

tive region sitting at even lower energy. The basic cell is repeated for 30 to 40 periods in order to enhance the output power.
Quantum cascade lasers have been built on the InGaAs/InAlAs systems (lattice matched to InP) and GaAs/AlGaAs one (lattice matched to GaAs) [24–27]. They are usually n-type and operate in the range 5-20 μm, with output power of the order of few mW, under CW conditions (at least of to 200 K) or under pulsed condition up toroom temperature and higher. Weak electro luminescence in the THz regime (above 5 THz) has been reported in [28–30]. Recently, two Monte Carlo simulations have indicated that it is possible to achieve population inversion and lasing action in this regime. One of the analyses [31] was based on a conventional QCL with a 2-well active region.
Population inversion is achieved up to 77 K with an electric field of about 35 kV/cm.
The second con-sidered a SL GaAs/AlGaAs QCL [32], with well width of 22 nm. An experimental verification of the THz QCLs was announced [33] recently. The laser works at 4.4 THz with an output power of 2 mW up to a temperature of 45 K.
More recently progress in the filed has been rapid with experimental results achieved at 3.4 and 2.3 THz [34,35].

Stressed p-Ge Lasers

A candidate for tunable THz generation would have been the cryogenic p-Ge "hot hole" laser that emits broadband THz radiation resulting from transitions between the light- and heavy hole bands [39]. However, the large excitation power needed to obtain "streaming motion" of holes under crossed magnetic and electric fields prevents CW operation. More recently, it has been observed that for p-Ge under large uni-axial external pressure, laser action occurs at moderate excitation powers, without the need of a magnetic field [36]. The proposed population inversion mechanism is illustrated in fig.a [40, 37]. Under uni-axial pressure the light- and heavy hole sub-bands split up and, for P > 2.5 kbar // [100] and P > 4 kbar // [111], the acceptor ground state connected with the heavy hole band enters the continuum of the light hole sub-band and becomes a so-called resonant state. Under impact ionisation conditions, the scattering of the holes at this resonant state results in a trapping of the holes near this state, leading to a maximum of the non-equilibrium hole distribution function near this energy [42].

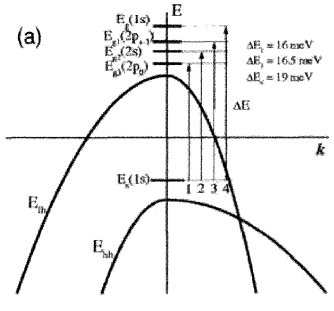

Fig.5. Energy level scheme showing the heavy hole 1s resonant state in the light hole con-

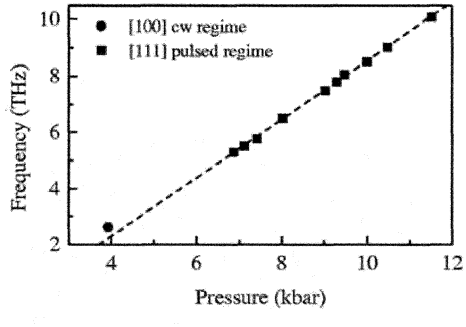

Fig. 6. Pressure dependence of the frequency of the main emission peak in stressed p-Ge [40]

tinuum + possible laser transitions [40]

Lasing action occurs between this resonant state and the bound ground- and excited states of the acceptor connected to the light hole sub-band, as shown in fig. 5.[40].
Frequency tuning between from 2.5–10 THz is possible by changing the pressure (fig. 6). The low excitation voltage needed to reach laser action proves that in this case, contrary to the p-Ge hot hole laser, no streaming motion of the holes is necessary to create a population inversion. Due to heating, for bias voltages above 10V/cm only pulsed operation is possible at a mW power level. For lower voltages CW operation at the microwatt level has been observed at 2.5 THz with a lasing threshold excitation power of only 10 mW [38, 41].

Conclusions and Further Work

The novel photomixing scheme presented in this paper is believed to be the only way forward in improving THz performance of photomixers, as a result of this study. In order to introduce the advantages of this scheme a detailed, and lengthy, explanation of photomixer physics and state-of-the-art performance was hardly avoidable. The other two technologies presented, THz QCLs and p-Ge lasers, are thought to be equally promising and their development is ongoing without this study. Presently, the second phase of this ESA study has begun for some time and has focused on the realisation of the superlattice photodiode as well as the duplication of the THz QCL and p-Ge results reported in the literature. Emphasis is also put on QCL modelling in order to better understand the ultimate theoretical limitations, in terms of lower frequency and operating temperatures.

References

[1] J.J.A. Baselmans, M. Hajenius, J.R. Gao, P.A.J. de Korte, T.M. Klapwijk, B. Voronov, G. Gol'tsman, "Noise Performance of NbN Hot Electron Bolometer Mixers at 2.5 THz and its Dependence on the Contact Resistance", Published in these Proceedings.

[2] P. Khosropanah, S. Bedorf, S. Cherednichenko, K. Jacobs, H.F. Merkel, E. Kollberg, "Fabrication and Noise Measurement of NbTiN Hot Electron Bolometer Heterodyne Mixers at THz Frequencies", Published in these Proceedings.

[3] H.F. Merkel, P. Khosropanah, S. Cherednichenko, E. Kollberg, "Comparison of the Noise Performance of NbTiN and NbN Hot Electron Bolometer Heterodyne Mixers at THz Frequencies", Published in these Proceedings.

[4] R. Teipen, M. Justen, T. Tils, S. Glenz, C. E. Honingh, K. Jacobs, B.D. Jackson, T. Zijlstra, M. Kroug, "Influence of Junction Quality and Current Density on HIFI Band 2 Mixer Performance", Published in these Proceedings.

[5] W. Jellema, P. Wesselius, S. Withington, G. Yassin, J.A. Murphy, C. O'Sullivan, N. Trappe, T. Peacocke, B. Leone, "Experimental Verification of Electromagnetic Simulations of a HIFI Mixer Sub-Assembly", Published in these Proceedings.

[6] J. Baubert, M. Salez, P. Khosropanah, S. Cherednichenko, H.F. Merkel, "A Hot-Spot Model for Membrane-Based HEB", Published as Poster in these Proceedings.

[7] M. Hajenius, J.J.A. Baselmans, J.R. Gao, T.M. Klapwijk, P.A.J. de Korte, "Current-Voltage and Resistance-Temperature characteristics of Nb(Ti)N Phonon Cooled HEB Mixers With and Without Contact Resistance", Published as Poster in these Proceedings.
[8] H.F. Merkel, "NbAu Bilayer Diffusion Cooled HEB – Model versus Experiment, Published as Poster in these Proceedings.
[9] N. Erickson, R. Grosslein, J. Wielgus, V. Fath, "An All Solid State Source for 1.7 THz", Published in these Proceedings.
[10] J. Ward, F. Maiwald, A. Maestrini, G. Chattopadhyay, E, Schlecht, J. Gill, I. Mehdi, "1400–1900 GHz Local Oscillators for the Herschel Space Observatory", Published in these Proceedings.
[11] E.R. Brown, et al., APL 66, 4903 (1995).
[12] S. Matsuura et al., "A travelling-wave THz photomixer based on angle-tuned phase matching", Appl. Phys. Lett. **74**, 2872 (1999).
[13] S. Matsuura et al., "Design and characterization of optical-THz phase-matched travelling wave photomixers", Proceedings of SPIE 3795, 484 (1999).
[14] E.K. Duerr et al., "Distributed photomixers", Proceedings of CLEO, CWU6 (2000).
[15] E.K. Duerr, "Distributed photomixers", PhD Thesis, Massachusetts Institute of Technology, September 2002.
[16] N. Shimizu, et al., Jpn. J. Appl. Phys. **37**, 1424 (1998).
[17] N. Shimizu, et al., Jpn. J. Appl. Phys. **38**, 2573 (1999).
[18] H. Ito, T. Ito, Y. Muramoto, T. Furuta, T. Ishibashi, "F-Band (90-140 GHz) Uni-Traveling-Carrier Photodiode Module for a Photonic Local Oscillator", Published in these Proceedings.
[19] C. Kadow, et al., Physica E **7**, 97 (2000).
[20] M. Eckardt, et al., Proceedings of HCIS12 (2001), Physica **B 314**, 154 (2002).
[21] A. Schwanhäußer, et al., Proceedings of HCIS12 (2001), Physica **B 314**, 273 (2002).
[22] J. Faist, F. Capasso, D. L. Sivco, C. Sirtori, A. L. Hutchinson, and A. Y. Cho, Science, **264**, 553 (1994).
[23] G. Scamarcio, F. Capasso, C. Sirtori, J. Faist, A.L. . Hutchinson, D. L. Sivco, and A. Y. Cho, Science, **276**, 773 (1997).
[24] F. Capasso, C. Gmachl, R. Paiella, A. Tredicucci, A. L. Hutchinson, D. L. Sivco, J. N. Baillargeon, A. Y. Cho, and H. C. Liu, IEEE J. Sel. Top. Quantum Electron. **6**, 931 (2000).
[25] D. Hofstaetter, M. Beck, T. Aellen, J. Faist, U. Oesterle, M. Illegems, E. Gini, and H. Melchior, Appl. Phys. Lett. **78**, 1964 (2001).
[26] J. Faist, F. Capasso, D. L. Sivco, S. N. G. Chu, and A. Y. Cho, Appl. Phys. Lett. **72**, 680 (1998).
[27] A. Tredicucci, C. Gmachl, F. Capasso, D. L. Sivco, A. L. Hutchinson, and A. Y. Cho, Appl. Phys. Lett. **74**, 638 (1999).
[28] M. Rochat, J. Faist, M. Beck, U. Oesterle, and M. Ilegems, Appl. Phys. Lett. **73**, 3724 (1998).
[29] B. S. Williams, B. Xu, Q. Hu, and M. R. Melloch, Appl. Phys. Lett. **75**, 2927 (1999).

[30] J. Ulrich, R. Zobl, K. Unterrainer, G. Strasser, and E. Gornik, Appl. Phys. Lett. **76**, 19 (2000).
[31] R. Köhler, R.C. Iotti, A. Tredicucci, and F. Rossi, Appl. Phys. Lett. **79**, 3920 (2001).
[32] F. Compagnone, M. Manenti, and P. Lugli, Submitted for publication.
[33] R. Köhler, A. Tredicucci, F. Beltram, H.E. Beere, E.H. Linfield, A.G. Davies, D.A. Ritchie, R.C. Iotti, F. Rossi, Nature **417**, 156 (2002).
[34] B.S. Williams, H. Callebaut, S. Kumar, H. Qing, J.L. Reno, "TeraHertz Quantum Cascade Laser Based on LO-Phonon-Scattering Assisted Depopulation", Published in these Proceedings.
[35] G. Scalari. Private communication.
[36] I.V. Altukhov, E.G. Chorkova, M.S. Kagan, K.A. Korelev, V.P. Sinis, F.A. Smirnov, Sov. Phys. JETP 74(1992)404.
[37] "Resonant acceptor states and terahertz stimulated emissionof uniaxially strained germanium", I.V. Altukhov, M.S. Kagan, K.A. Korelev, V.P. Sinis, E.G. Chorkova, JETP 88(1999)51
[38] "Continuous stimulated THz emission due to intra-centre population inversion in uniaxially strained germanium", I.V. Altukhov, M.S. Kagan, , Yu. P. Gousev,, I.V. Altukhov, Physica B272(1999)458
[39] Opt. Quantum Electron. Vol. 23, Special Issue on Far-Infrared Semiconductor Lasers, edited by E. Gornik and A.A. Andronov (Chapman and Hall, London 1991)
[40] "Widely tunable continous-wave THz laser", Yu. P. Gousev, I.V. Altukhov, K.A. Korelev, V.P. Sinis, M.S. Kagan, E.E. Haller, M.A. Odnoblyudov, I.N. Yasseievich, K-A. Chao, Appl. Phys. Lett. 75(1999)757
[41] "Resonant acceptor states and stimulated THz emissionin semiconductors and semiconductor structures", M.S. Kagan, I.N. Yasseievich, Proceedings of the 11th Internat. Symposium on Ultrafast Phenomena in Semiconductors, Vilnius, 2001.
[42] "Population inversion induced by resonant states in semiconductors", M.A. Odnoblyudov, I.N. Yasseievich, M.S. Kagan, Yu. M. Galperin, K.A. Chao, Phys. Rev. Lett. 83(1999)644.